



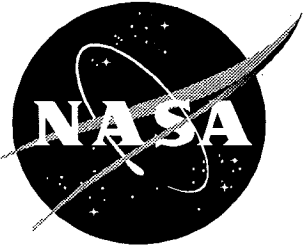
NASA Technical Paper 3594

1N-73
97784

Study of Analytic Statistical Model for Decay of Light and Medium Mass Nuclei in Nuclear Fragmentation

Francis A. Cucinotta and John W. Wilson

October 1996



Study of Analytic Statistical Model for Decay of Light and Medium Mass Nuclei in Nuclear Fragmentation

*Francis A. Cucinotta and John W. Wilson
Langley Research Center • Hampton, Virginia*

Available electronically at the following URL address: <http://techreports.larc.nasa.gov/ltrs/ltrs.html>

Printed copies available from the following:

NASA Center for AeroSpace Information
800 Elkridge Landing Road
Linthicum Heights, MD 21090-2934
(301) 621-0390

National Technical Information Service (NTIS)
5285 Port Royal Road
Springfield, VA 22161-2171
(703) 487-4650

Abstract

The angular momentum independent statistical decay model is often applied using a Monte-Carlo simulation to describe the decay of prefragment nuclei in heavy ion reactions. This paper presents an analytical approach to the decay problem of nuclei with mass numbers less than 60, which is important for galactic cosmic ray (GCR) studies. This decay problem of nuclei with mass number less than 60 incorporates well-known levels of the lightest nuclei ($A < 11$) to improve convergence and accuracy. A sensitivity study of the model level density function is used to determine the impact on mass and charge distributions in nuclear fragmentation. This angular momentum independent statistical decay model also describes the momentum and energy distribution of emitted particles (n , p , d , t , h , and α) from a prefragment nucleus.

Introduction

The description of heavy ion fragmentation is important for assessing damage to human cells and microelectronic equipment during spaceflight and on high-altitude airplane flights. Currently, few measurements of fragmentation cross sections are available because many collision pairs of interest exist for assessing the full galactic cosmic ray (GCR) spectrum interacting with various materials of interest. Other reasons include the unavailability of heavy ion accelerators and the high cost of measurement programs. Physical models (ref. 1) of heavy ion reactions must instead be used to provide databases for radiation transport codes (ref. 2) from which damage assessment may be made.

Heavy ion fragmentation is usually described as a two-step process of abrasion-ablation. Abrasion describes the geometric overlap of two nuclei and the accompanying loss of material (nucleons) in the overlap region, with the size of this region dependent on the impact parameter of the collision. The large piece of nuclear matter remaining after the abrasion step is called the prefragment nucleus. Ablation occurs when the prefragment nucleus is in a state of excitation and decays by particle emission to a stable configuration. The abrasion step is described by using geometric pictures (refs. 1 and 3) or optical models (refs. 4 and 5), and more recently with quantum models (refs. 6 and 7). The ablation step is described in the geometric picture (ref. 1) with the Rudstam charge distribution formulas and in the optical model approach with Monte-Carlo codes (refs. 8 and 9) for the statistical decay of an equilibrated system.

Development of nuclear databases for GCR studies requires reaction models that are computationally efficient and accurate. References 6 and 10 detail efficient computational procedures for describing the abrasion step of the reaction. The present report describes the analytic solution to the statistical decay model (refs. 11–13) and a sensitivity study of available nuclear level density models.

Statistical decay codes are often applied to a large number of nuclei, including ones with very large mass number A ($A > 60$), which are not of interest in GCR studies. This report focuses on a restricted range of nuclei typical of the prefragments formed during GCR fragmentation and uses analytic methods that are easily coupled to abrasion and excitation energy models. This approach incorporates the well-known levels of the lighter mass nuclei ($A \leq 12$) and applies the statistical decay model to heavier mass nuclei. The statistical approach examines the decay (or evaporation cascade) of heavier mass prefragments ($A > 11$), along with the decay at higher energies of some lighter mass nuclei where the decay properties are not well-known. The energy and momentum spectra of the emitted particles (n , p , d , t , h , and α) during decay are also represented consistently in the same statistical model.

This report also describes the analytic solutions for fragment formation from an initial excited nucleus and the energy and momentum spectrum of the emitted or evaporated light ions. Physical inputs are then described, and numerical examples of the models are presented.

Statistical Decay Model for Residual Nuclei Formation

In the classical theory of statistical decay, the probability that a nucleus a with excitation energy E_a^* will decay by emitting a particle j with kinetic energy E_j is given by (refs. 11 and 13)

$$P_j^a(E_j) = \frac{2\mu_{jb}g_jE_j}{\sum_i F_i^a} \sigma_{bj} w_0^b(E_a^* - S_j^a - E_j) \quad (1)$$

where g_j is the statistical weight (listed in table 1), σ_{bj} is the formation cross section, μ_{jb} is the reduced mass M of j and the residual nucleus b in $a \rightarrow b + j$, and S_j^a is the separation energy given by

$$S_j^a = M_j + M_b - M_a \quad (2)$$

(We use subscripts j, k, l, \dots to label the light ions emitted in a decay and superscripts a, b, c, \dots to label the parent and daughter nuclei.) In equation (1), w_0^b is the level density of the residual nucleus at the residual excitation energy $E_b^* = E_a^* - S_j^a - E_j$. Also, in equation (1) F_j^a is the total probability for emitting j from a given by

$$F_j^a = \int_0^{E_a^* - S_j^a} P_j^a(E) dE \quad (3)$$

which satisfies the condition

$$\sum_j F_j^a = 1 \quad (4)$$

where the summation is over the types of particles which may be emitted at a given excitation energy. The actual values of input parameters for describing the probability function are described in the "Formation Cross Sections and Decay Probability" section of this report. The present development is independent of these values; others could be used. Mass conservation and charge number conservation lead to

$$A_a = A_b + A_j \quad (5)$$

$$Z_a = Z_b + Z_j \quad (6)$$

The probability of emitting j and forming a stable residual nucleus b depends on the residual excitation energy and the separation energies of b , denoted by S_k^b . If the excitation energy is below the minimum separation energy of the residual nucleus, no further decays are possible, which implies a stable b :

$$E_b^* = E_a^* - S_j^a - E_j \leq \min[S_k^b] \quad (7)$$

For an unstable b ,

$$E_b^* = E_a^* - S_j^a - E_j > \min[S_k^b] \quad (8)$$

For charged particle emission the conditions in equations (7) or (8) must be modified to include the Coulomb barrier. The total probability F_j^a at excitation energy E_a^* is divided into two parts corresponding to formation of a stable or unstable residual nucleus as

$$F_j^a = G_j^a + H_j^a \quad (9)$$

where the probability of forming a stable residual nucleus is given by

$$G_j^a = \int_{E_a^* - S_j^a - \min[S_k^b]}^{E_a^* - S_j^a} P_j^a(E) dE \quad (10)$$

and the probability of forming an unstable residual nucleus is given by

$$H_j^a = \int_0^{E_a^* - S_j^a - \min[S_k^b]} P_j^a(E) dE \quad (11)$$

For sufficiently high initial excitation energy E_a^* several to many decays may occur; this occurrence leads to an evaporation cascade. In the statistical model the individual steps are treated as largely independent and connected only through the conservation of energy, mass, and charge. The evaporation cascade can be represented by using a master equation (ref. 12), with the development herein representing a perturbative solution to this equation.

The possibility of a second decay occurs for $E_b^* > \min[S_k^b]$, and the probability of forming a stable nucleus from b is given by

$$G_{jk}^{ab} = \int_0^{E_a^* - S_j^a - \min[S_k^b]} P_j^a(E) dE \int_{E_a^* - S_j^a - S_k^b - E}^{E_a^* - S_j^a - S_k^b} P_k^b(E') dE' \quad (12)$$

with similar expressions for higher order terms. We approximate the second and higher order terms in the evaporation cascade by introducing the average energies of E_j in emission to form stable residuals given by

$$\bar{E}_j^G = \int_{E_a^* - S_j^a - \min[S_k^b]}^{E_a^* - S_j^a} E P_j^a(E) dE \quad (13)$$

and unstable residuals given by

$$\bar{E}_j^H = \int_0^{E_a^* - S_j^a - \min[S_k^b]} E P_j^a(E) dE \quad (14)$$

The probability of forming a stable residual nucleus with $A_c = A_a - A_j - A_k$ and $Z_c = Z_a - Z_j - Z_k$ after two decays is then approximated by

$$G_{jk}^{ab} \approx H_j^a(E_a^*) G_k^b(E_a^* - S_j^a - \bar{E}_j^H) \quad (15)$$

and a stable residual nucleus with $A_d = A_a - A_j - A_k - A_l$ and $Z_d = Z_a - Z_j - Z_k - Z_l$ after three decays by

$$G_{jkl}^{abc} = H_j^a(E_a^*) H_k^b(E_a^* - S_j^a - \bar{E}_j^H) G_l^c(E_a^* - S_j^a - S_k^b - \bar{E}_j^H - \bar{E}_k^H) \quad (16)$$

with similar expressions for higher order terms. The number of terms in the cascade series depends on the initial excitation energy and the number of decay particles j allows. Early Monte-Carlo studies

(ref. 13) suggest that for nuclei in the mass range of the GCR ($A < 60$) the probability of evaporation of particles heavier than ${}^4\text{He}$ is small. Nuclear structure effects on the separation energies reduce the likelihood of emission of the mass 2 and 3 ions, especially for $A > 20$, although structure effects may play a role in some cases. Table 2 presents the number of terms in the decay series for emission of n , p , and α with emission of n , p , d , t , h , and α , which is clearly a slowly converging series for large prefragment mass ($A > 20$) and high initial excitation energy.

Spectrum of Light Ions

The spectrum of emitted ions j is found by summing the contributions of the j ions from single, double, and so forth, evaporations until the initial excitation energy is exhausted. Keeping track of the excitation energy available in the decay probability functions by introducing the notation

$$P_j^a(E_a^*, E_j) = P_j^a(E_j) \quad (17)$$

for equation (1) allows the cumulative spectrum to be written as

$$\begin{aligned} \frac{dN_j}{dE} = & P_j^a(E_a^*, E) + \sum_k \int_0^{E_a^* - S_k^a - S_j^b} dE' P_k^a(E_a^*, E') P_j^b(E_a^* - S_k^a - E', E) \\ & + \sum_k \sum_l \int_0^{E_a^* - S_k^a - S_l^b} dE' \int_0^{E_a^* - S_k^a - S_l^b - S_j^c - E'} dE'' P_k^a(E_a^*, E') P_l^b(E_a^* - S_k^a - E', E'') \\ & \times P_j^c(E_a^* - S_k^a - S_l^b - E' - E'', E) + \dots \end{aligned} \quad (18)$$

The higher order terms in equation (18) correspond to high initial excitation energy. At high excitation energy, the statistical decay properties (as discussed in the section "Results and Discussion") will change slowly. An approximation of equation (18) similar to the one used in equations (15) and (16) is then found as

$$\begin{aligned} \frac{dN_j}{dE} = & P_j^a(E_a^*, E) + \sum_k H_k^a(E_a^*) P_j^b(E_a^* - S_k^a - \bar{E}_k^H, E) \\ & + \sum_k \sum_l H_k^a(E_a^*) H_l^b(E_a^* - S_k^a - \bar{E}_k^H) P_j^c(E_a^* - S_k^a - S_l^b - \bar{E}_k^H - \bar{E}_l^H, E) + \dots \end{aligned} \quad (19)$$

Assuming isotropic emission, the momentum distribution in the rest frame of the initial nucleus is found as

$$\frac{dN_j}{d\mathbf{p}} = \frac{1}{4\pi} \frac{1}{pE} \frac{dN_j}{dE} \quad (20)$$

In heavy ion fragmentation the prefragment nuclei are produced with a velocity or momentum recoil spectrum in the first stage of the reaction. The recoil spectrum is expected to be well represented by a Gaussian function and is denoted by $f(\mathbf{v} - \mathbf{v}_0)$, where \mathbf{v}_0 is the velocity vector of the primary nucleus, $\mathbf{v}_0 = 0$ for target fragmentation, and $\mathbf{v}_0 \approx \mathbf{v}_p$, where \mathbf{v}_p is the projectile velocity vector for projectile fragmentation. The invariant momentum distribution in the lab or projectile rest frame is then

$$E_j' \frac{dN_j}{d\mathbf{p}_j'} = \int d\mathbf{v} f(\mathbf{v} - \mathbf{v}_0) E_j \frac{dN_j}{d\mathbf{p}_j} \quad (21)$$

where primed values refer to the laboratory or projectile frame and

$$E_j = \gamma_v (E'_j - \beta_v p'_j \cos \theta'_j) \quad (22)$$

where γ_v and β_v are functions of v and v_0 .

Formation Cross Sections and Decay Probability

Following Dostrovsky (refs. 13 and 14), the energy dependence of the formation cross sections, the effects of tunneling, and the Coulomb barrier are simulated by using the following method:

For neutrons,

$$\sigma_n = \pi R_j^2 \alpha_n \left(1 + \frac{\beta_n}{E_n} \right) \quad (23)$$

with

$$\alpha_n = 0.76 + 2.2 A_b^{-1/3} \quad (24)$$

$$\beta_n = \frac{1}{\alpha_n} (2.22 A_b^{-2/3} - 0.05) \quad (25)$$

and

$$R_j = 1.5 A_b^{-1/3} \quad (26)$$

For charged ions,

$$\sigma_j = \pi R_j^2 \alpha_j \left(1 - \kappa_j \frac{B_j^a}{E_j} \right) \quad (27)$$

with the Coulomb barrier given by

$$V_{jb} = \frac{Z_b Z_j e^2}{R_b + \rho_j} \quad (28)$$

The parameters α_j , κ_j , and ρ_j are given by Dostrovsky (ref. 14) for $Z_b \geq 10$ and are extrapolated linearly to lower Z_b herein.

In the statistical model, the level density at $E_a^* - S_j^a - E_j$ is approximated by (ref. 13)

$$w_0^b(E^* - S_j^a - E_j) \approx w_0^b(E^*) e^{-(E_j + S_j^a)/\tau_j^b} \quad (29)$$

where τ_j^b is the nuclear temperature defined by

$$\tau_j^b = \left\{ \frac{d \ln [w_0^b(E)]}{dE} \right\}^{-1} \quad (30)$$

The decay probability function is then rewritten in the form

$$P_j^a(E_j) = A_j^a(E_j - B_j^a) w_0^b(E_a^*) e^{-(E_j + S_j^a)/\tau_j^b} \theta(E_j - \kappa_j V_{bj}) \quad (31)$$

where

$$A_j^a = \frac{2\mu_j b g_j \pi R_j^2 \alpha_j}{\sum_i F_i^a} \quad (32)$$

and

$$B_j^a = \begin{cases} \beta_n & (j = n) \\ -\kappa_j V_{bj} & (j \neq n) \end{cases} \quad (33)$$

The functions F_j^a , G_j^a , and H_j^a then have solutions of the form

$$I_j^a = A_j^a w_0^b(E_a^*) \int_{E_1}^{E_2} (E_j - B_j^a) e^{-(E_j + S_j^a)/\tau_j^b} dE_j \quad (34)$$

$$I_j^a = A_j^a w_0^b(E_a^*) \tau_j^b \left[e^{-(E_2 + S_j^a)/\tau_j^b} (B_j^a - E_2 - \tau_j^b) - e^{-(E_1 + S_j^a)/\tau_j^b} (B_j^a - E_1 - \tau_j^b) \right] \quad (35)$$

with $E_1 = B_j^a$, if $E_1 < B_j^a$ for $j \neq n$. Similarly, the average energy of the emitted particles \bar{E}_j^G and \bar{E}_j^H can also be found in closed form.

In calculations, the separation energies and masses of the particles are evaluated by using experimental values from reference 15. A large number of decays may occur for high excitation energies. The function G_j^a approaches zero at high E^* , whereas H_j^a becomes almost constant. Calculations are shown in the section "Results and Discussion;" however, first we discuss models of the level density function.

Models for Level Density Function

The level density function can be derived from an equidistant spacing model that assumes all one-particle states are equally spaced. The level density then takes the form (ref. 16)

$$w_0(A, Z, E^*) = \frac{\sqrt{\pi} e^S}{12 E^{*5/4} a^{1/4}} \quad (36)$$

where a is the level density parameter and S the entropy, which is expressed as

$$S = 2\sqrt{aE^*} \quad (37)$$

In the Fermi gas model, the level density parameter is related to the spacing parameter d by (ref. 16)

$$a = \frac{\pi^2}{6d} \quad (38)$$

with d expressed in terms of the Fermi energy ϵ_F and mass number A by

$$d = \frac{2\epsilon_F}{3A} \quad (39)$$

The values used for the level density parameter found in the literature often range from $a = A/8 \text{ MeV}^{-1}$ to $a = A/20 \text{ MeV}^{-1}$.

To account for important deviations from the equidistant spacing model such as pairing effects, shell structure, and energy gaps, the excitation energy in equation (36) is often replaced by an effective excitation energy, and the level density parameter is allowed to have a dependence on the excitation energy. The model of Ignatyuk, Smirenkin, and Tishin (ref. 17) uses the form

$$S^2 = 4\bar{a} \left[E^* - \Delta_p - \Delta_n + \Delta E_{\text{shell}} \left(1 - e^{-\gamma E^*} \right) \right] \quad (40)$$

where Δ_p and Δ_n are the proton and neutron pairing corrections, respectively, and ΔE_{shell} is the ground state shell correction given by

$$\Delta E_{\text{shell}} = M_{\text{exp}} - M_{LD} \quad (41)$$

where M_{exp} is the experimental mass and M_{LD} is the mass corresponding to the liquid drop model. The pairing correction is taken as

$$\Delta_{n \text{ or } p} = \begin{cases} \frac{12 \text{ MeV}}{A^{1/2}} & (\text{if } n \text{ or } p \text{ is odd}) \\ 0 & (\text{if } n \text{ or } p \text{ is even}) \end{cases} \quad (42)$$

The level density parameter is written as

$$\bar{a} = A(c_1 + c_2 A) \quad (43)$$

Several modifications to equation (40) have also been considered (ref. 16), including studies where the parameters c_1 , c_2 , and γ are fit to slow neutron and proton resonances for most nuclei or a restricted range of mass numbers. The equation of state corresponding to equation (40) is

$$E^* - \Delta_p - \Delta_n = \bar{a} \left(1 + \Delta E_{\text{shell}} \frac{1 - e^{-\gamma E^*}}{E^*} \right) \tau^2 \quad (44)$$

Several other corrections to the level density model and decay parameters can also be considered. These include use of a limiting temperature to restrict states with short-lived lifetimes that are not expected to decay statistically. (See ref. 18.) Also, temperature-dependent masses and Coulomb barriers are often introduced at high excitation energies. (See refs. 13 and 19.) These corrections can be studied in this model by modification of input parameters.

Results and Discussion

The use of an average residual energy of the daughter nuclei to replace the integral over the energy spectrum of emitted ions is the main approximation used to reduce the evaporation cascade to a more convergent summation of terms. To test this approximation, figure 1 presents calculations using the approximate expressions and approximations using numerical integration for the evaporation spectrum of n , p , d , and α ions from ^{19}F . Terms corresponding to three decays at several initial excitation energies are shown. The approximate solutions work well, and similar results are found with other nuclei.

To increase the accuracy and convergence of the evaporation cascade, the functions F_j^a , G_j^a , and H_j^a for lighter mass nuclei ($A < 11$) are replaced by experimental values (refs. 20–22) up to the highest known excitation energies where the statistical model is used at higher excitation energies. The statistical model agrees reasonably well at low excitation energy for higher mass numbers. Figures 2–5 show

the functions G and H versus excitation energy for a representative number of nuclei. In most cases the functions G_j^a are small above $E^* = 50$ MeV, and the functions H_j^a are fairly constant above 100 MeV. This behavior allows the use of $G_j^a \approx 0$ in the evaporation cascade at high excitation energies (>100 MeV) and improves convergence in the code.

To consider the effect of the level density model employed when calculating predicted fragmentation cross sections, the abrasion-ablation model is used to consider the effects on elemental and mass distributions for realistic cases. The abrasion cross sections are calculated in the abrasion model of Townsend et al. (refs. 5 and 23) with numerical techniques described by Cucinotta, Townsend, and Wilson (ref. 10). Here the elemental distribution is given by

$$\sigma_{Z_F} = \sum_{A_F} \sum_{A_F^*} \sum_{Z_F^*} \alpha_{F, F^*} \sigma_{ABR}(A_F^*, Z_F^*, E_F^*) \quad (45)$$

and the mass distribution by

$$\sigma_{A_F} = \sum_{Z_F} \sum_{A_F^*} \sum_{Z_F^*} \alpha_{F, F^*} \sigma_{ABR}(A_F^*, Z_F^*, E_F^*) \quad (46)$$

where the parameter α_{F, F^*} represents a cumulative $G_{jkl}^{abc\dots}$ function that results in the formation of a fragment F from the prefragment F^* .

In the present calculations, the excitation energies of the prefragments are from the NUCFRG code (refs. 1 and 24), which gives two excitation energies for each prefragment corresponding to surface and frictional excitation energies at two trajectories. Figures 6–10 show elemental and mass distributions for several projectile nuclei interacting with ^{12}C targets. References 25–27 present experimental data for elemental production cross sections. Calculations are shown that use the level density function of equation (36) in the equidistant spacing model with $a = A/8 \text{ MeV}^{-1}$. Calculations including pairing and shell corrections using the effective excitation energy (eq. (43)) noted in reference 17 are also shown. The equidistant spacing model without the level density corrections is in poor agreement with the experiment for most odd Z fragments. In contrast, use of the effective excitation energy leads to fairly good agreement for the projectiles studied for both even Z and odd Z fragments. Large differences between the two models for the level density are also seen in the mass distribution of fragments.

The present abrasion model needs further corrections for elastic fragmentation and excitation of low level states which decay through gamma-ray emission to improve the agreement for fragments produced with masses near that of the projectile. Here the NUCFRG model does not consider the actual separation energies, and with removal of a few nucleons the excitation energies may be mismatched with realistic models of level spectrum. Microscopic approaches to define the excitation energy spectrum of the prefragment nuclei must be developed to improve predictive capability and identify shortcomings in the statistical decay model.

The calculations in this report for fragmentation of projectile nuclei with $A_P < 28$ have a CPU time under 5 minutes on a VAX-4000 series computer. As mass removal increases, prefragment excitation energies exceed 200 MeV and the number of prefragments grows dramatically. The required CPU time for ^{40}Ar is about 2 hours and for ^{56}Fe about 8 hours. Here a Monte-Carlo simulation of the evaporation cascade would be more useful. However, the convergence of the analytic approach may be improved by neglecting d , t , and h emissions, which greatly reduces the number of cascade terms for large numbers of decays (high excitation energies). The importance of d , t , and h emissions is expected to be reduced for $A_F^* > 20$ because of the increased separation energies of these ions compared to p , n , and α separation energies. Figure 10 presents elemental distributions for three or six decay particles for ^{20}Ne , ^{40}Ar , and ^{56}Fe fragmentation. The truncation to three decay particles (n , p , and α) appears to be fairly

accurate for heavier ions such as ^{40}Ar and ^{56}Fe . A hybrid model using six ions for excitation energies below about 100 MeV and three ions for excitation energies above 100 MeV for the heavier prefragments is clearly suggested.

Concluding Remarks

Improvement in the database for heavy ion fragmentation cross sections is the primary area of physics research for development of radiation transport codes for cosmic ray studies. The correct physical description for developing models of these reactions is the two-step model of abrasion-ablation. Past research has not focused on describing the ablation step when developing heavy ion fragmentation data bases. This report shows that an analytic formalism of the statistical decay model provides reliable results when using the abrasion-ablation model. Furthermore, the model shows that the nuclear level density used in the calculations has a major effect in predicting secondary mass and charge production cross sections. The approach developed in this report can be extended to aid the development of a complete database for galactic cosmic ray radiation transport codes. Improving physical inputs to the calculations should be considered, and improved convergence methods for the evaporation cascade at large excitation energies in the mass 25–45 region should be developed.

NASA Langley Research Center
Hampton, VA 23681-0001
July 16, 1996

References

1. Wilson, John W.; Townsend, Lawrence W.; and Badavi, F. F.: A Semiempirical Nuclear Fragmentation Model. *Nucl. Instrum. & Methods Phys. Res.*, vol. B18, no. 3, Feb. 1987, pp. 225–231.
2. Wilson, John W.; Townsend, Lawrence W.; Schimmerling, Walter; Khandelwal, Govind S.; Khan, Ferdous; Nealy, John E.; Cucinotta, Francis A.; Simonsen, Lisa C.; Shinn, Judy L.; and Norbury, John W.: *Transport Methods and Interactions for Space Radiations*. NASA RP-1257, 1991.
3. Bowman, J. D.; Swiatecki, W. J.; and Tsang, C. F.: *Abrasion and Ablation of Heavy Ions*. LBL-2908, Univ. of California, July 1973.
4. Hüfner, J.; Schäfer, K.; and Schürmann, B.: Abrasion-Ablation in Reactions Between Relativistic Heavy Ions. *Phys. Rev. C*, vol. 12, no. 6, Dec. 1975, pp. 1888–1898.
5. Townsend, L. W.; Wilson, J. W.; Cucinotta, F. A.; and Norbury, J. W.: Comparison of Abrasion Model Differences in Heavy Ion Fragmentation—Optical Versus Geometric Models. *Phys. Rev. C*, vol. 34, Oct. 1986, pp. 1491–1494.
6. Cucinotta, Francis A.; and Dubey, Rajendra R.: Alpha-Cluster Description of Excitation Energies in $^{12}\text{C}(^{12}\text{C}, 3\alpha)\chi$ at 2.1A GeV. *Phys. Rev. C*, vol. 50, no. 2, Aug. 1994, pp. 1090–1096.
7. Cucinotta, F. A.; Wilson, J. W.; Shinn, J. L.; and Tripathi, R. K.: Assessment and Requirements of Nuclear Reaction Data Bases for GCR Transport in the Atmosphere and Structures. *31st Scientific Assembly of COSPAR*, July 1996, p. 325.
8. Guthrie, Miriam P.: *EVAP-4: Another Modification of a Code To Calculate Particle Evaporation From Excited Compound Nuclei*. ORNL-TM-3119, U. S. Atomic Energy Commission, Sept. 10, 1970.
9. Morrissey, D. J.; Oliveira, L. F.; Rasmussen, J. O.; Seaborg, G. T.; Yariv, Y.; and Fraenkel, Z.: Microscopic and Macroscopic Model Calculations of Relativistic Heavy-Ion Fragmentation Reactions. *Phys. Rev. Lett.*, vol. 43, no. 16, Oct. 1979, pp. 1139–1142.
10. Cucinotta, Francis A.; Townsend, Lawrence W.; and Wilson, John W.: *Target Correlation Effects on Neutron-Nucleus Total, Absorption, and Abrasion Cross Sections*. NASA TM-4314, 1991.
11. Weisskopf, V. F.; and Ewing, D. H.: On the Yield of Nuclear Reactions With Heavy Elements. *Phys. Rev.*, vol. 57, Mar. 1940, pp. 472–485.
12. Campi, X.; and Hüfner, J.: Nuclear Spallation-Fragmentation Reactions Induced by High-Energy Projectiles. *Phys. Rev. C*, vol. 24, no. 5, Nov. 1981, pp. 2199–2209.

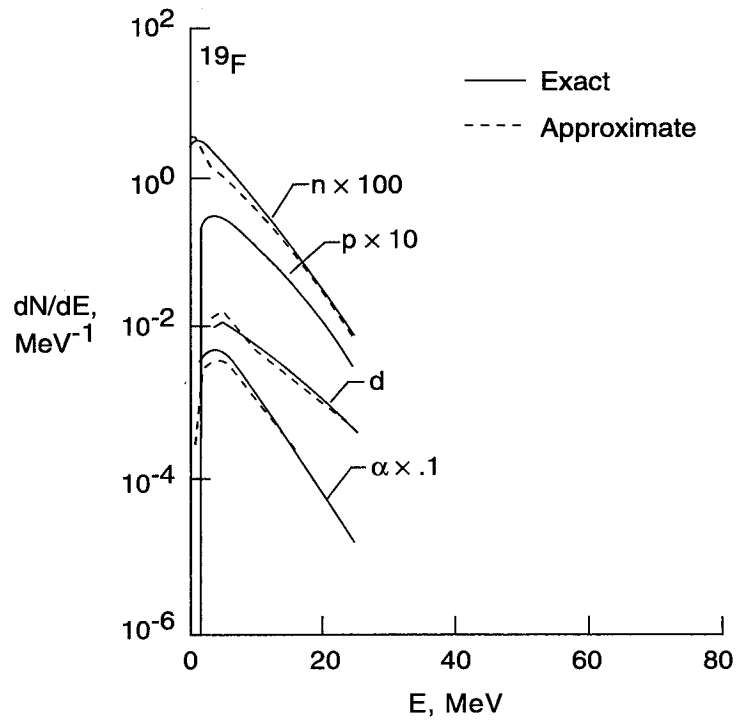
13. Kikuchi, Ken: *Nuclear Matter and Nuclear Reactions*. North-Holland Publ. Co, 1968.
14. Dostrovsky, I.; Fraenkel, Z.; and Friedlander, G.: Monte Carlo Calculations of Nuclear Evaporation Processes. III—Applications to Low-Energy Reactions. *Phys. Rev.*, vol. 116, no. 3, Nov. 1959, pp. 683–702.
15. Audi, G.; and Wapstra, A. H.: The 1993 Atomic Mass Evaluation. I—Atomic Mass., *Nucl. Phys. A*, vol. 565, no. 1, Dec. 1993, pp. 1–65.
16. Gadioli, Ettore; and Hodgson, P. E.: *Pre-Equilibrium Nuclear Reactions*. Oxford Univ. Press, 1992.
17. Ignatyuk, A. V.; Smirenkin, G. N.; and Tishin, A. S.: Phenomenological Description of the Energy Dependence of the Level Density Parameter. *Sov. J. Nucl. Phys.*, vol. 21, no. 3, 1975, pp. 255–257.
18. Fáti, George; and Randrup, Jørgen: Explosion-Evaporation Model for Fragment Production in Medium-Energy Nuclear Collisions. *Nucl. Phys.*, vol. A381, 1982, pp. 557–576.
19. De Angelis, A.; and Mekjian, A.: Models of Nuclear Fragmentation in Heavy-Ion Collisions. *Relativistic Heavy Ion Physics*, L. P. Csernai and D. D. Strottman, eds., World Scientific, 1991, pp. 364–405.
20. Ajzenberg-Selove, F.: Energy Levels of Light Nuclei A=5–10. *Nucl. Phys. A*, vol. 490, 1988, pp. 1–225.
21. Ajzenberg-Selove, F.: Energy Levels of Light Nuclei A=11–12. *Nucl. Phys. A*, vol. 506, no. 1, Jan. 1990, pp. 1–158.
22. Ajzenberg-Selove, F.: Energy Levels of Light Nuclei A=13–15. *Nucl. Phys. A*, vol. 523, no. 1, Feb. 1991, pp. 1–196.
23. Townsend, L. W.: *Optical-Model Abrasion Cross Sections for High-Energy Heavy Ions*. NASA TP-1893, 1981.
24. Wilson, J. W.; Shinn, J. L.; and Chun, S. Y.: NUCFRG2: A Semiempirical Nuclear Fragmentation Model. *Nucl. Instrum. & Methods Phys.*, vol. 94, nos. 1–2, Oct. 1994, pp. 95–102.
25. Webber, W. R.; Kish, J. C.; and Schrier, D. A.: Individual Isotopic Fragmentation Cross Sections of Relativistic Nuclei in Hydrogen, Helium, and Carbon Targets. *Phys. Rev. C*, vol. 41, no. 2, Feb. 1990, pp. 547–565.
26. Tull, C. E.: *Relativistic Heavy Ion Fragmentation at HISS*. LBL-29718, Univ. of California, Oct. 1990.
27. Sampsonidis, D.; Papanastassiou, E.; and Butsev, V. S.: Fragmentation Cross Sections of ^{16}O , ^{24}Mg , and ^{32}S Projectiles at 3.65 GeV/Nucleon. *Phys. Rev. C*, vol. 51, no. 6, June 1995, pp. 3304–3308.

Table 1. Light Ion Statistical Weights and Masses

Ion j	g_j	M_j , MeV
n	2	939.55
p	2	938.26
d	6	1875.58
t	6	2808.87
h	6	2808.34
α	4	3727.32

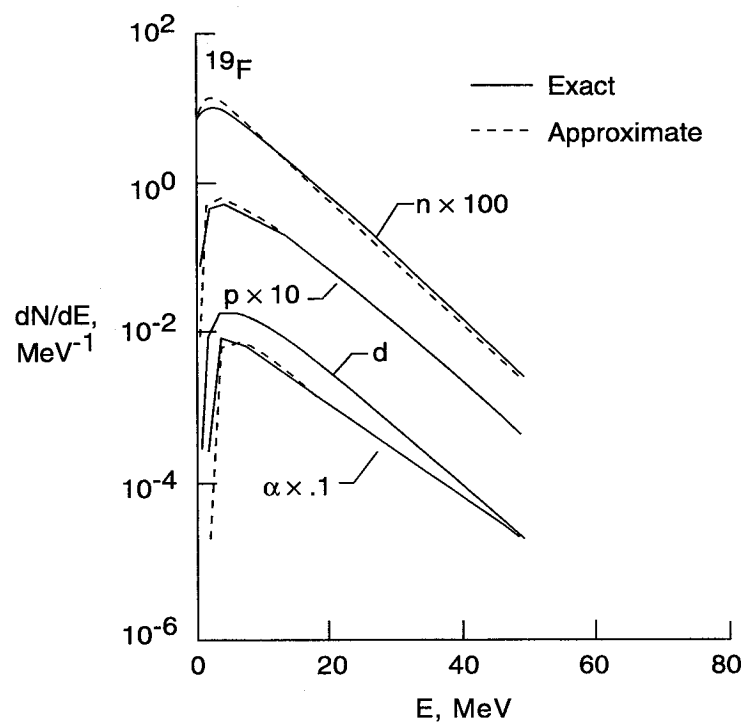
Table 2. Number of Terms (t_1 or t_2) for Number of Decays With 3 or 6 Decay Particles

Number of decays, N	t_1 (3 particles)	t_2 (6 particles)	t_2/t_1
1	3	6	2
2	9	36	4
3	27	216	8
4	81	1296	16
5	243	7 776	32
6	729	46 656	64
7	2 187	279 936	128
8	6 561	1 679 626	256
9	19 683	10 077 856	512



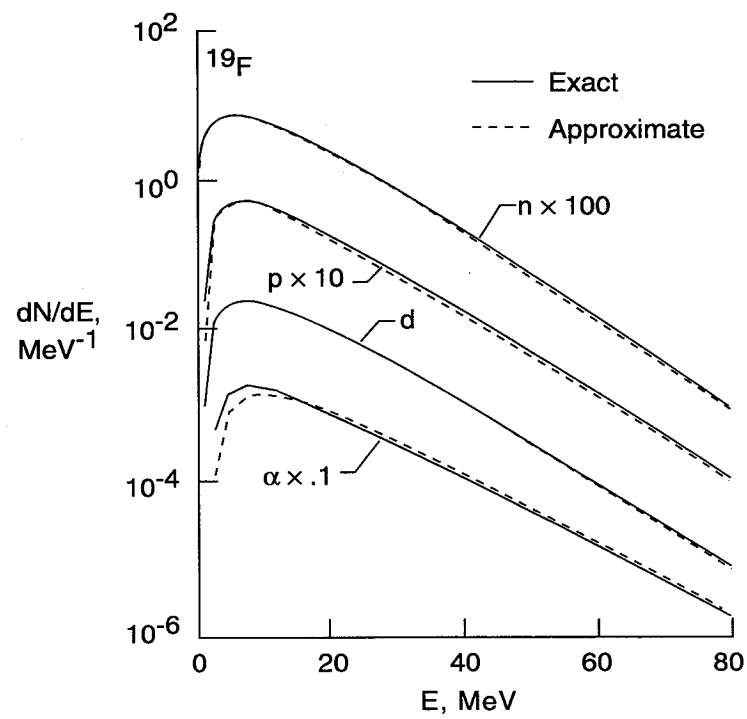
(a) $E^* = 25$ MeV.

Figure 1. Energy spectrum of evaporated particles from ^{19}F at different levels of MeV excitation energy using numerical integration of equation (18) and approximate solution of equation (19).



(b) $E^* = 50 \text{ MeV}$.

Figure 1. Continued.



(c) $E^* = 90 \text{ MeV}$.

Figure 1. Concluded.

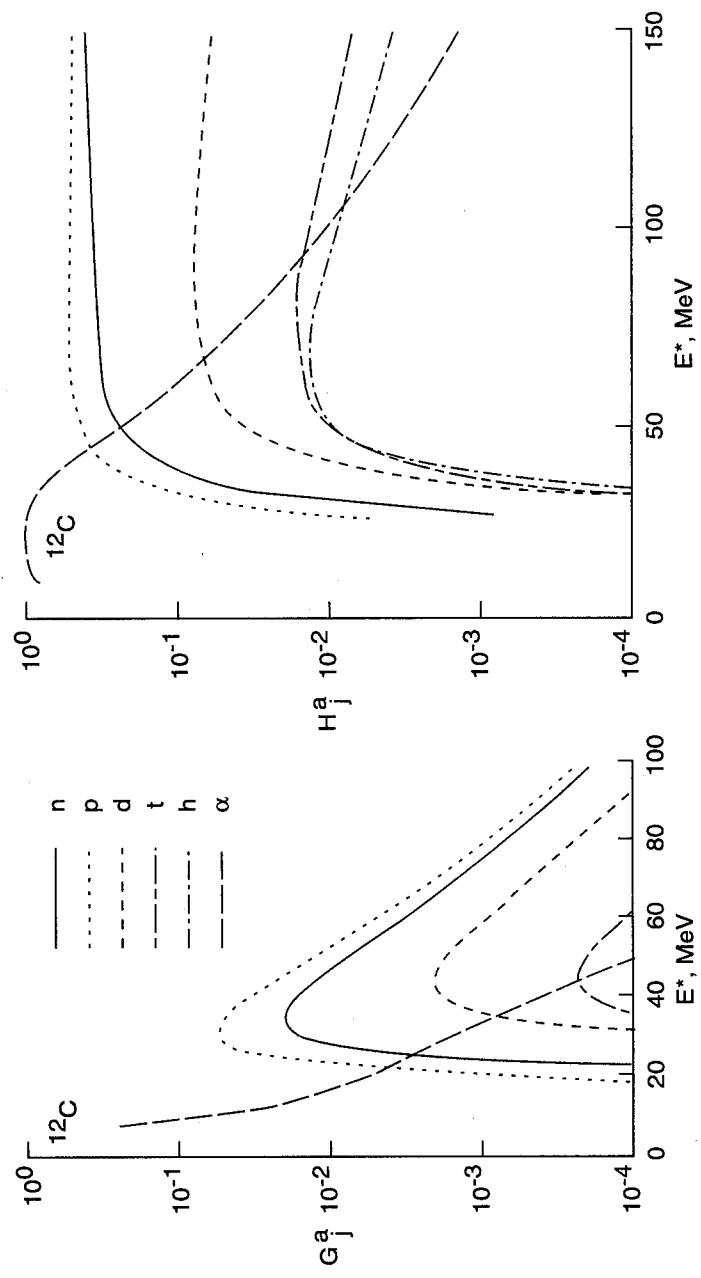
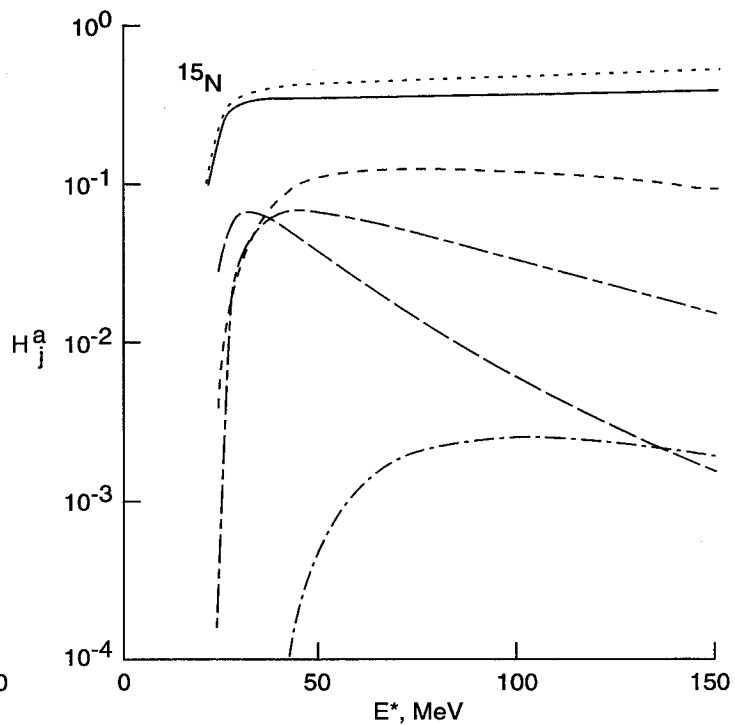
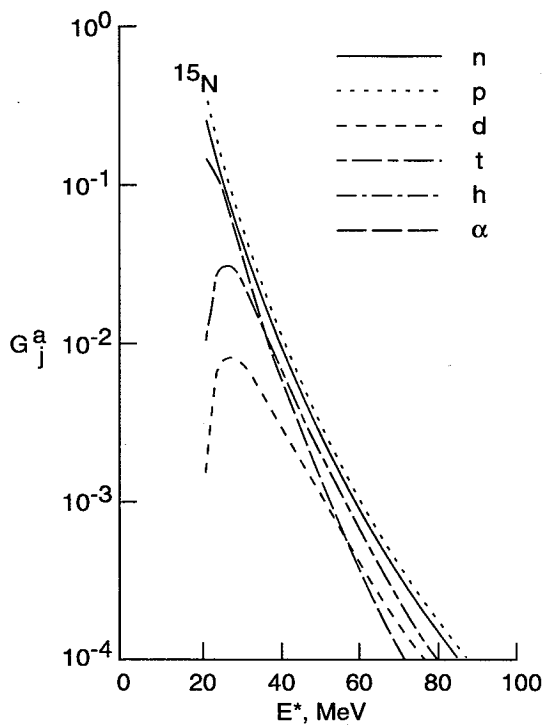
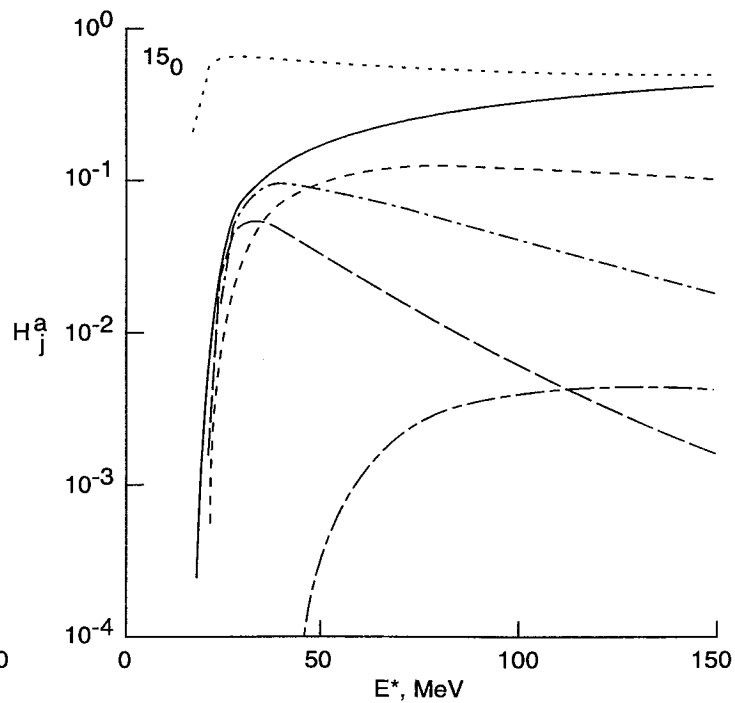
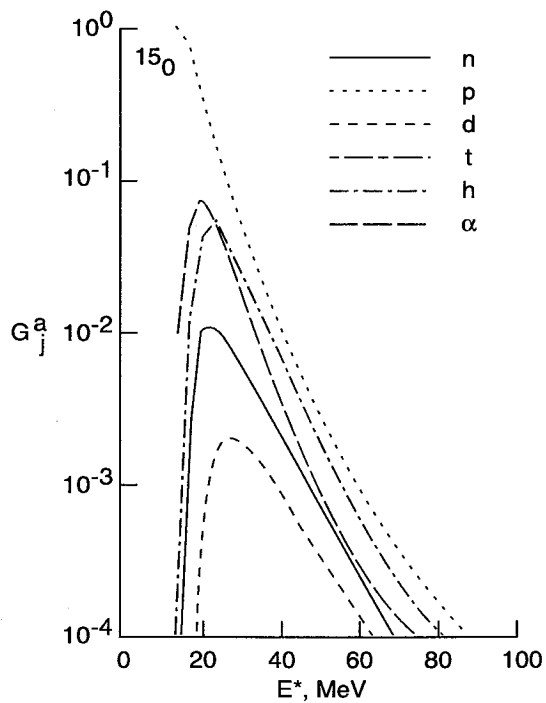


Figure 2. Calculations of G_j^a and H_j^a versus excitation energy for ^{12}C .

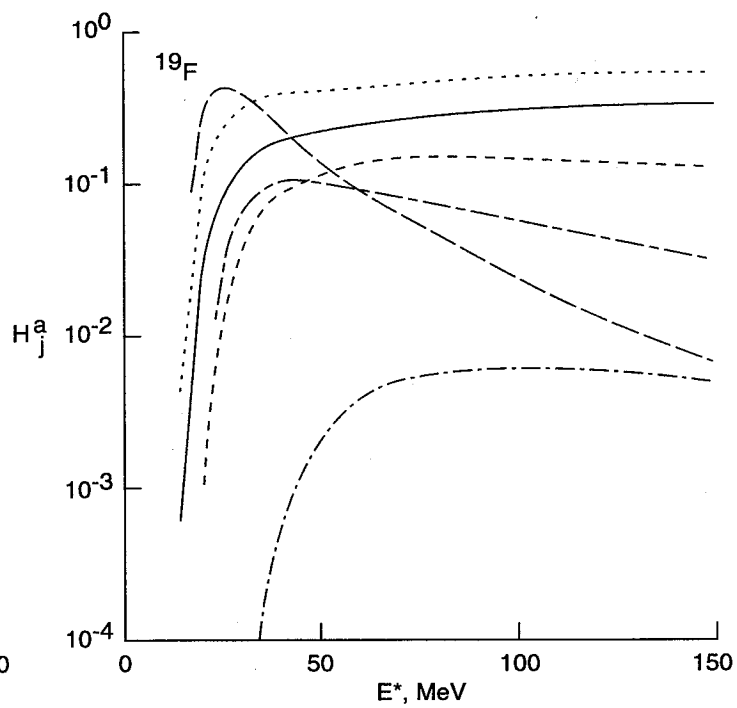
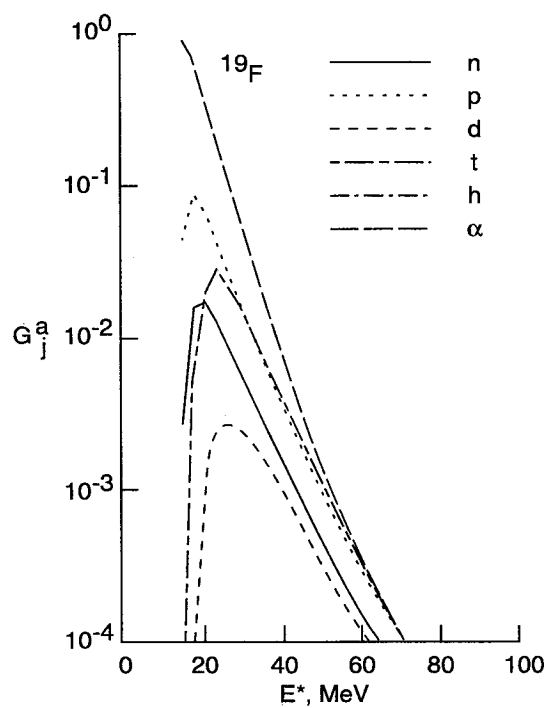


(a) ^{15}N .

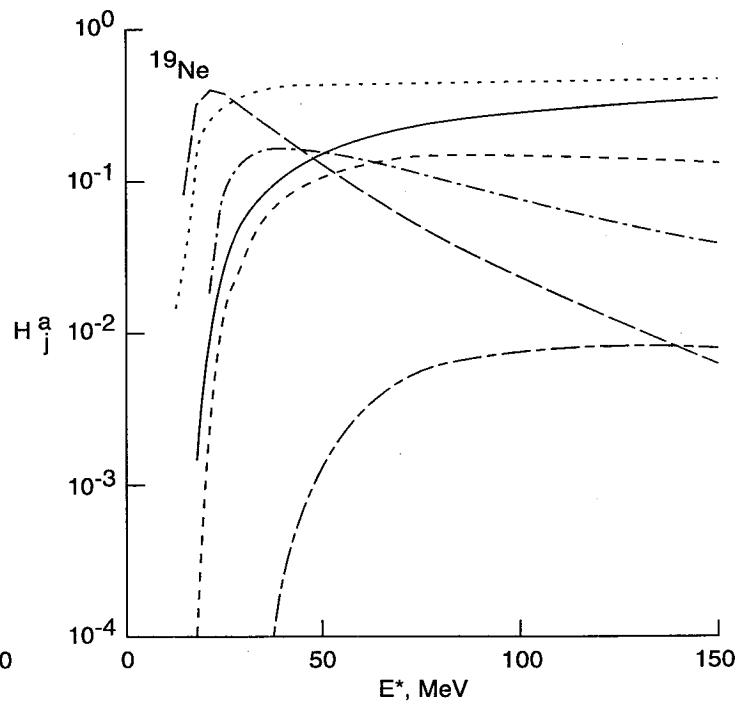
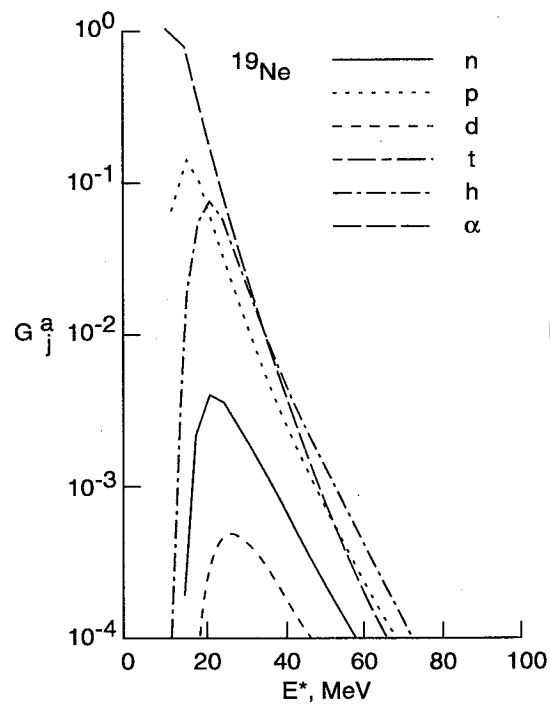


(b) ^{15}O .

Figure 3. Calculations of G_j^a and H_j^a versus excitation energy for ^{15}N and ^{15}O .

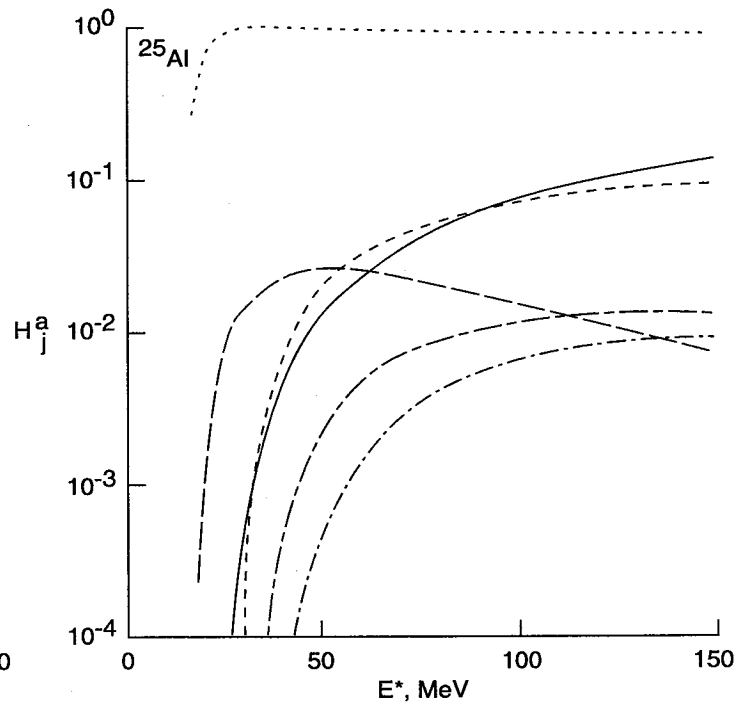
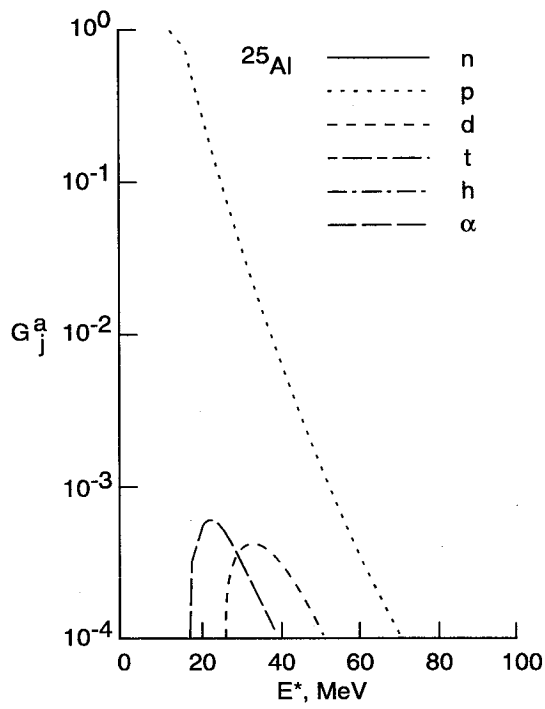


(a) ^{19}F .

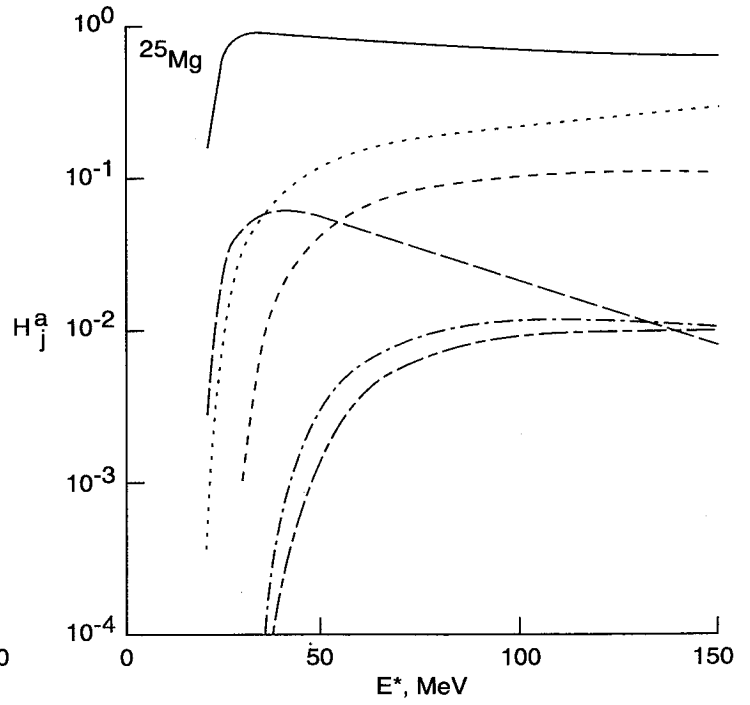
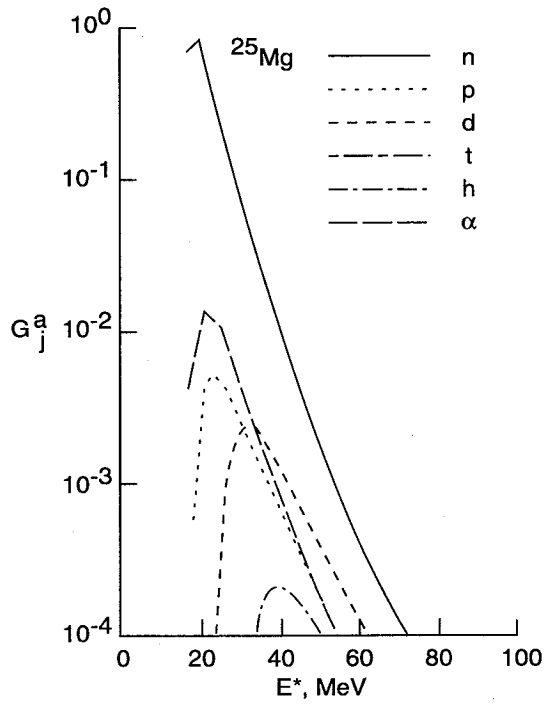


(b) ^{19}Ne .

Figure 4. Calculations of G_j^a and H_j^a versus excitation energy for ^{19}F and ^{19}Ne .

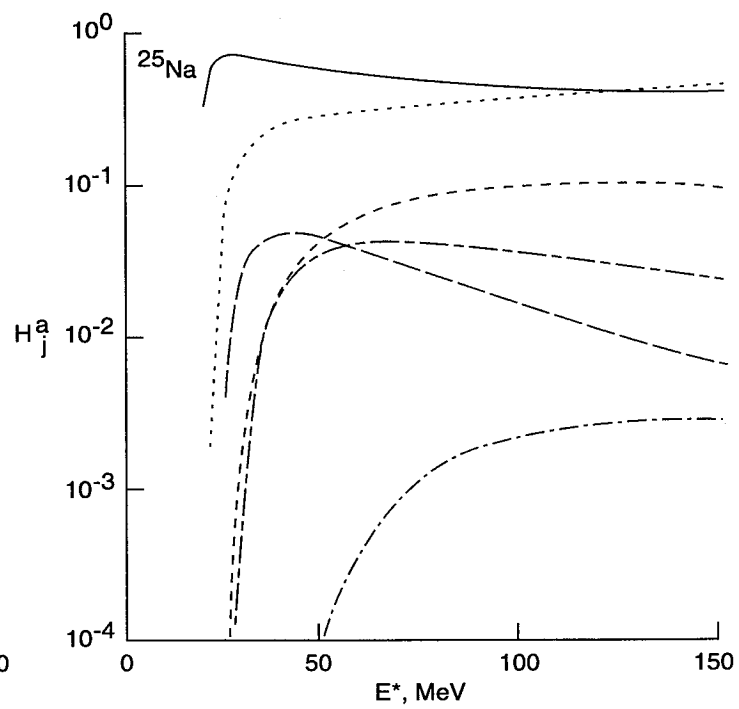
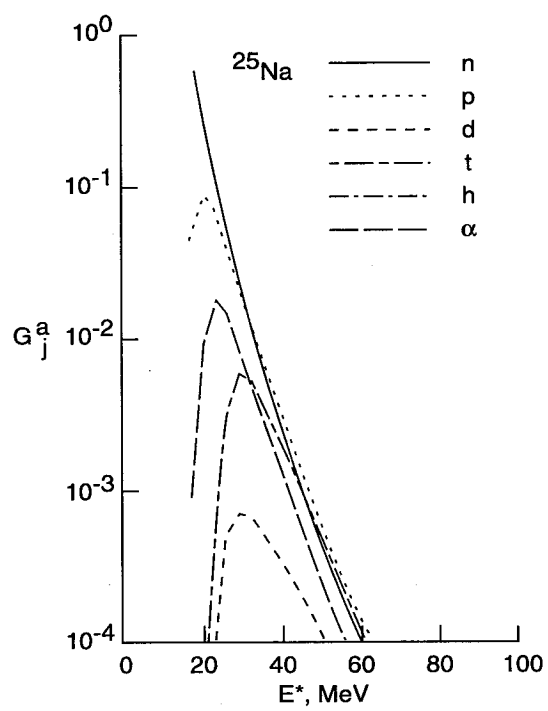


(a) ^{25}Al .



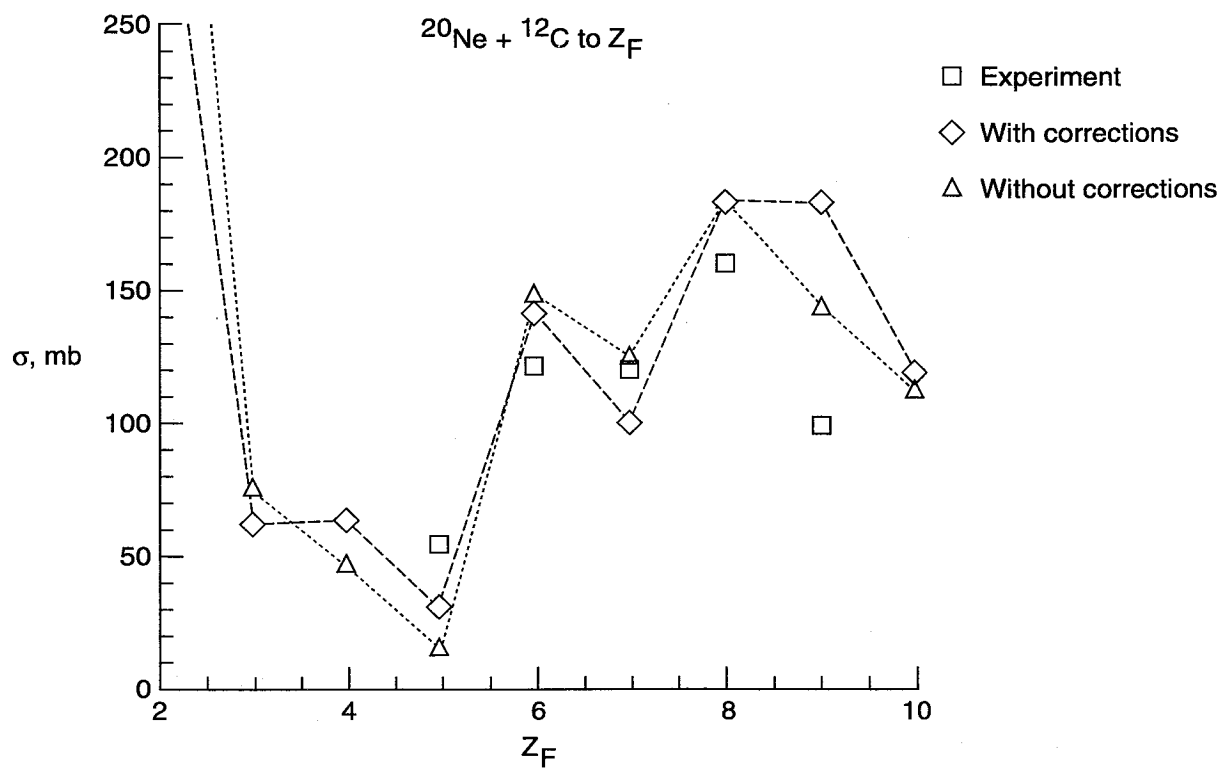
(b) ^{25}Mg .

Figure 5. Calculations of G_j^a and H_j^a versus excitation energy for ^{25}Al , ^{25}Mg , and ^{25}Na .

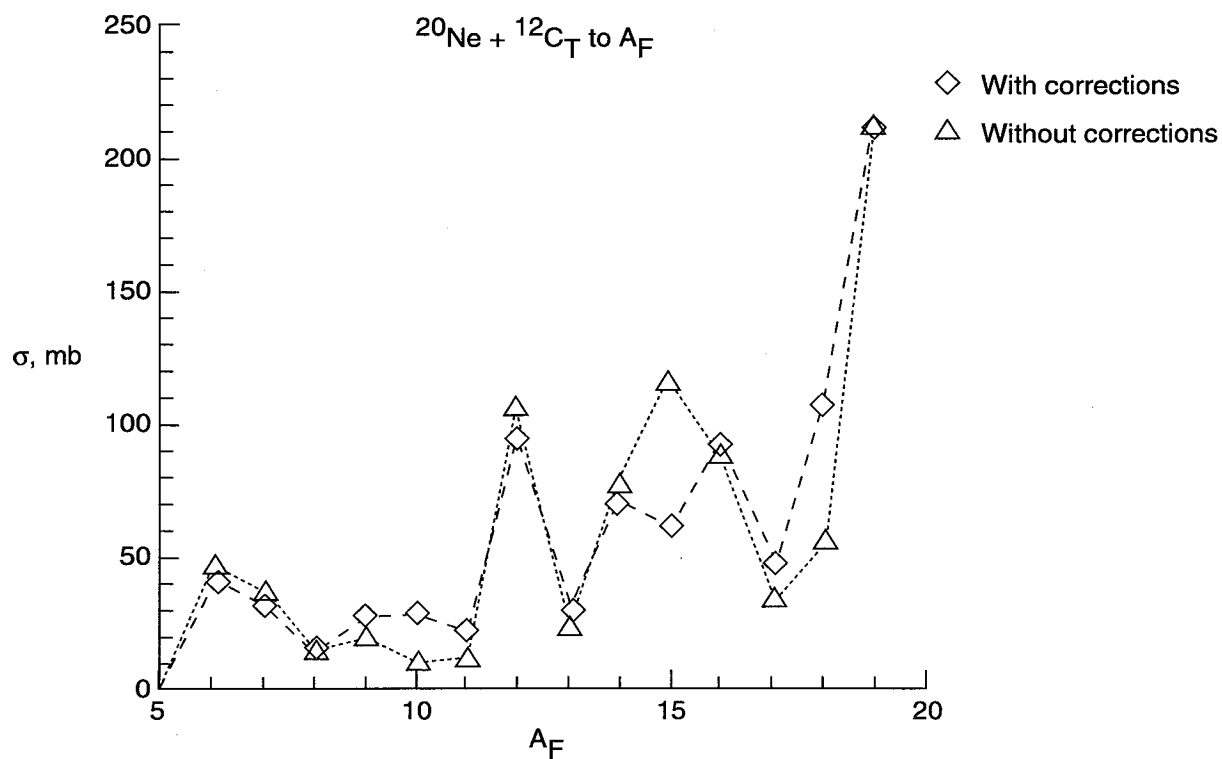


(c) ^{25}Na .

Figure 5. Concluded.

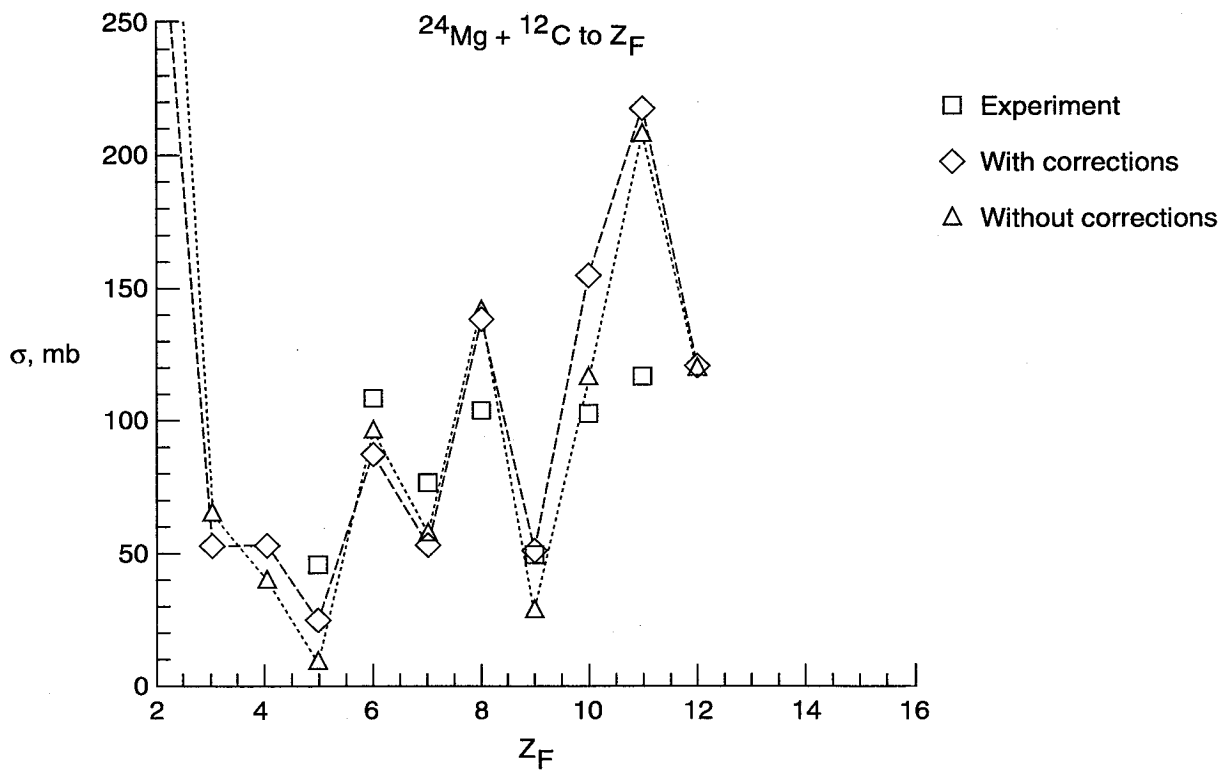


(a) Elemental production.

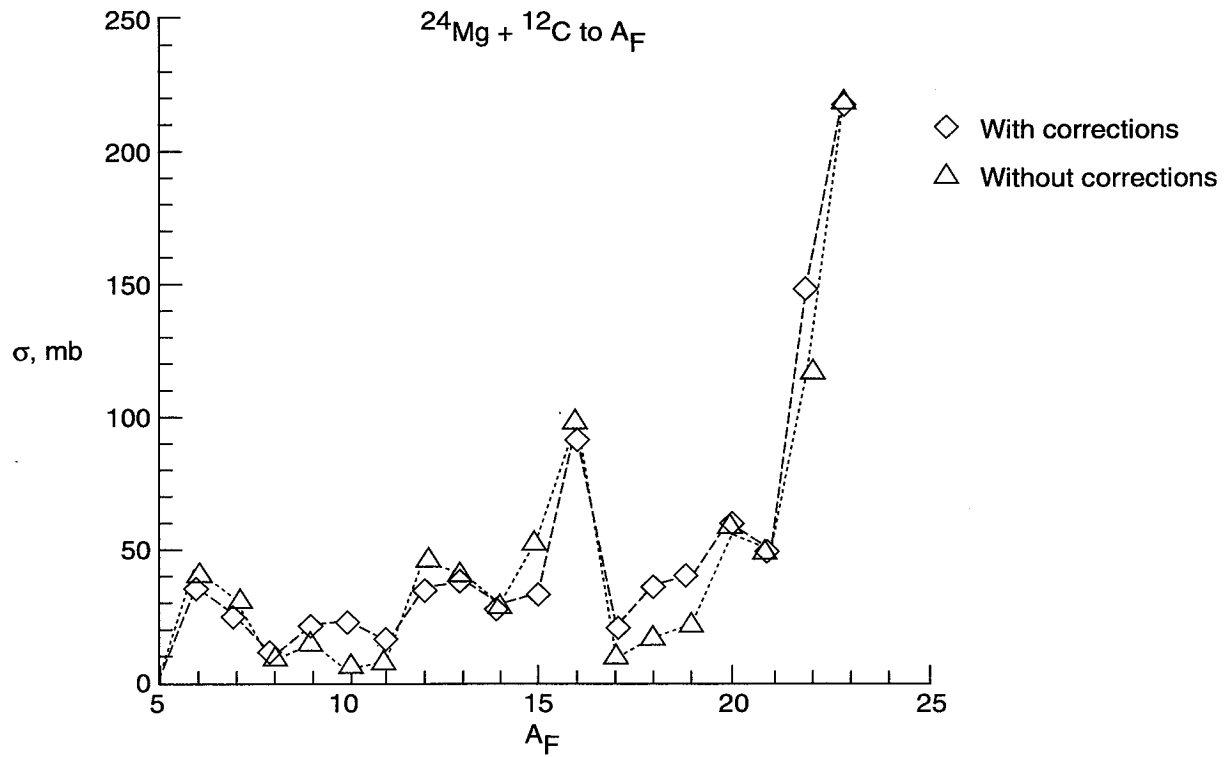


(b) Mass production.

Figure 6. Excitation energy cross section profiles for $^{20}\text{Ne} + ^{12}\text{C}$ at 0.6 GeV/amu.

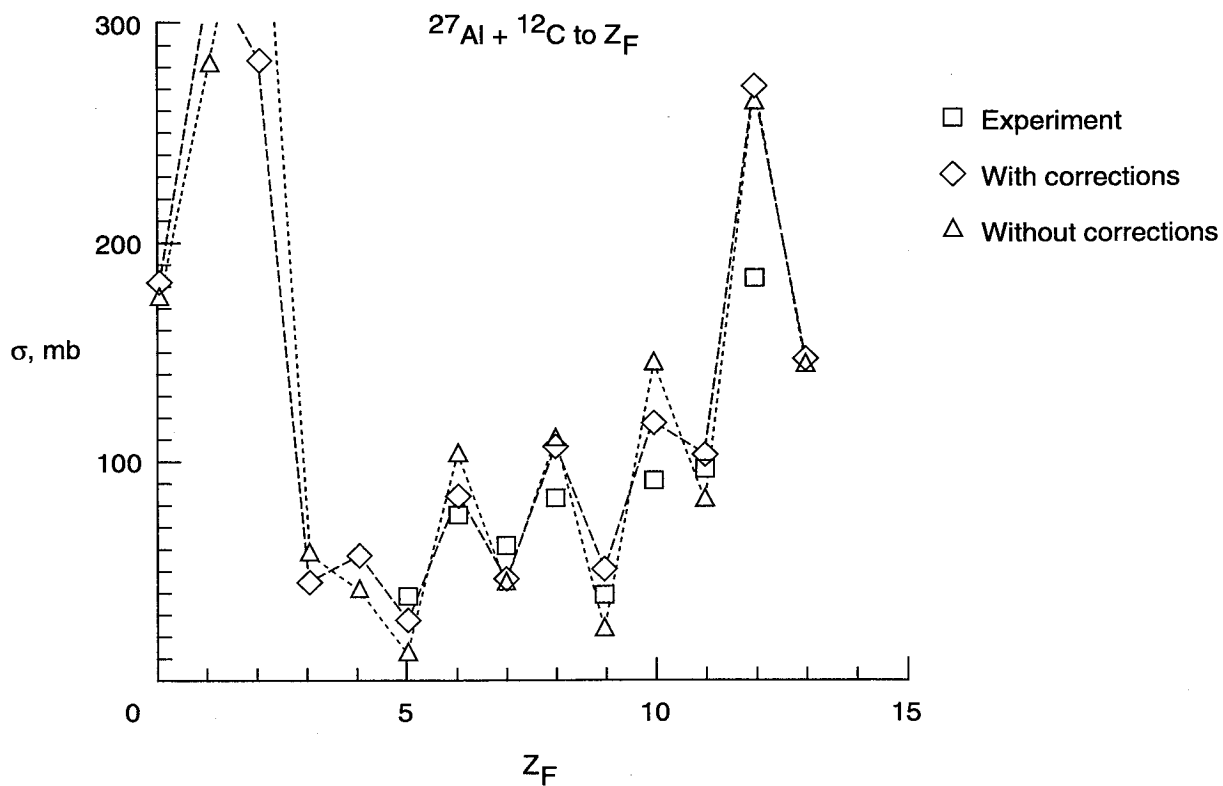


(a) Elemental production.

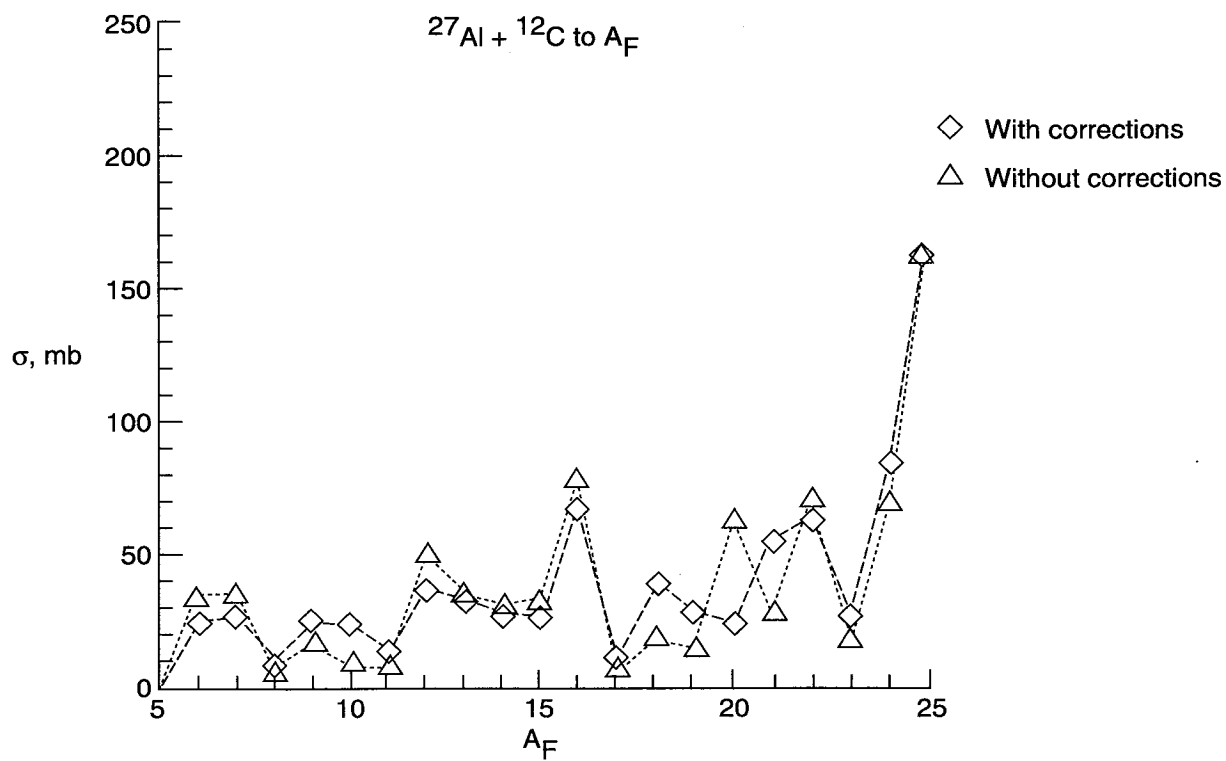


(b) Mass production.

Figure 7. Excitation energy cross section profiles for $^{24}\text{Mg} + ^{12}\text{C}$ at 0.74 GeV/amu.

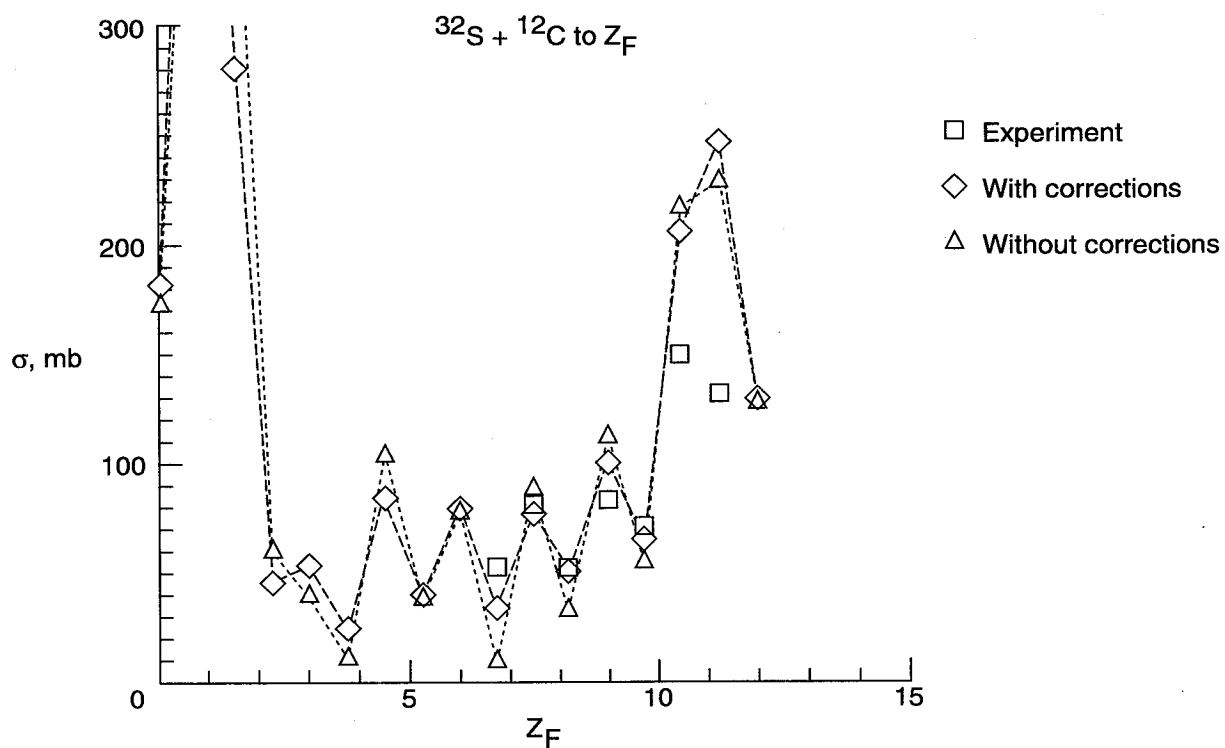


(a) Elemental production.

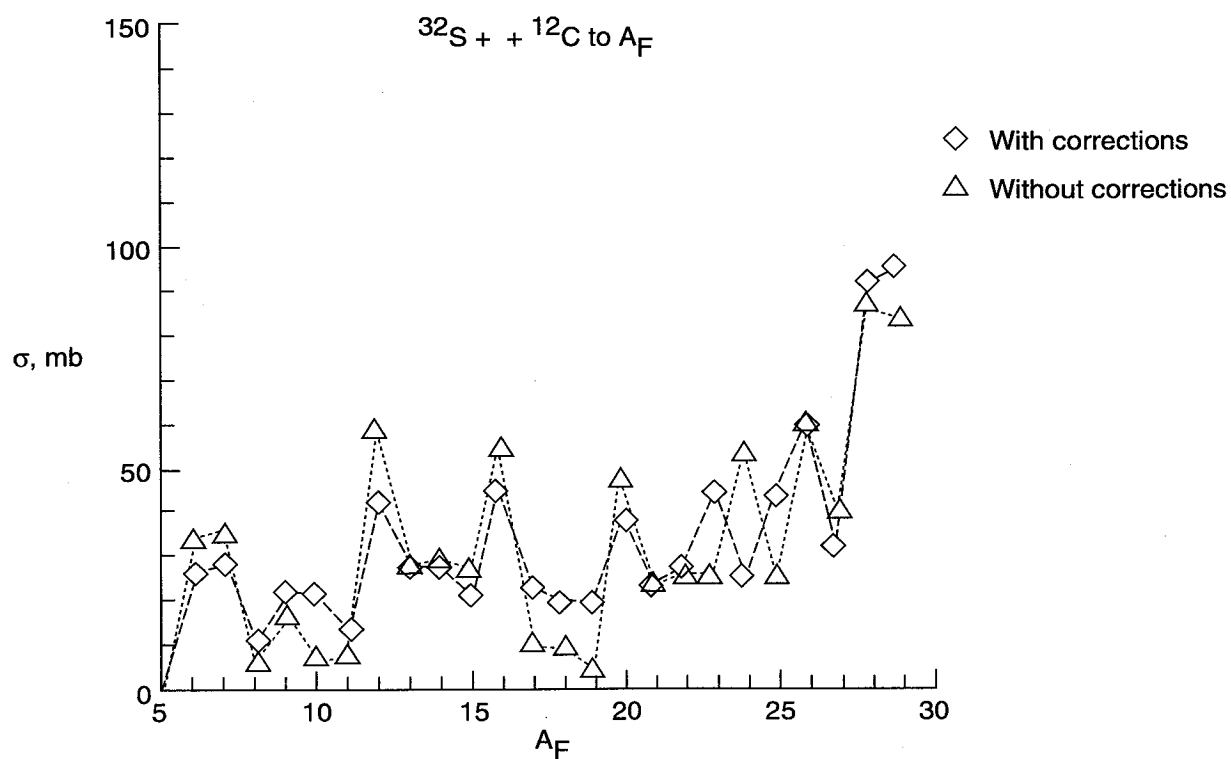


(b) Mass production.

Figure 8. Excitation energy cross section profiles for $^{27}\text{Al} + ^{12}\text{C}$ at 0.58 GeV/amu.



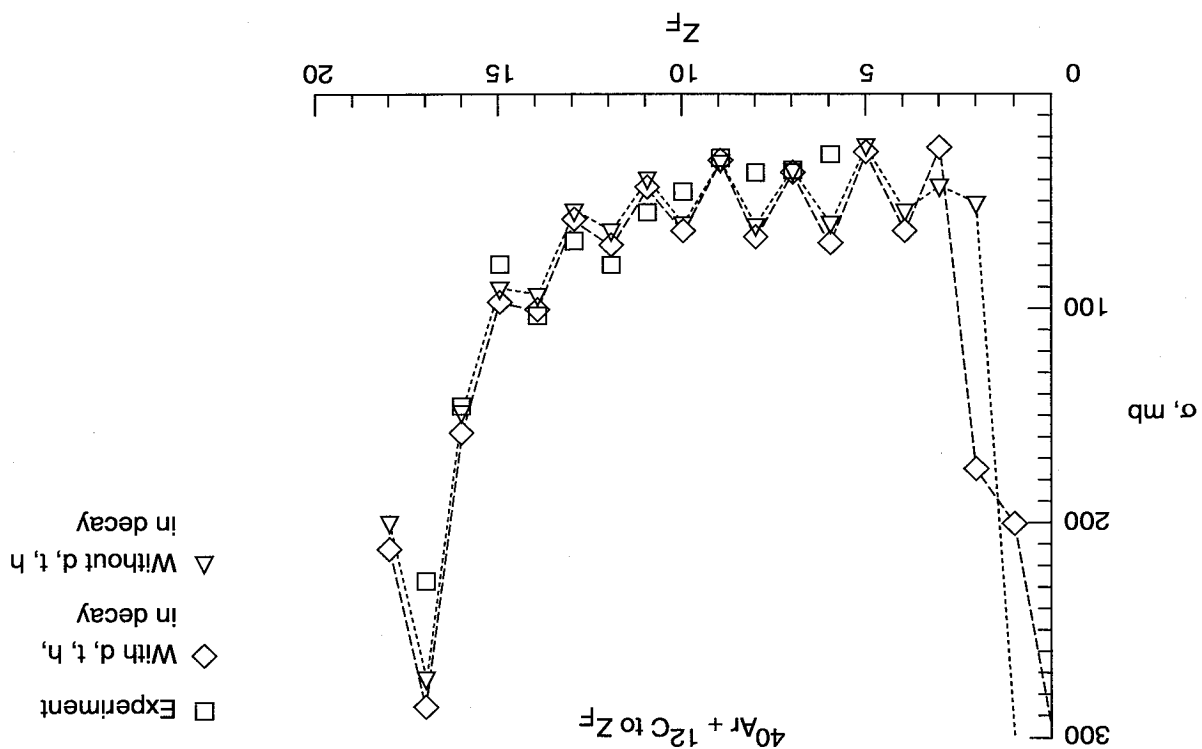
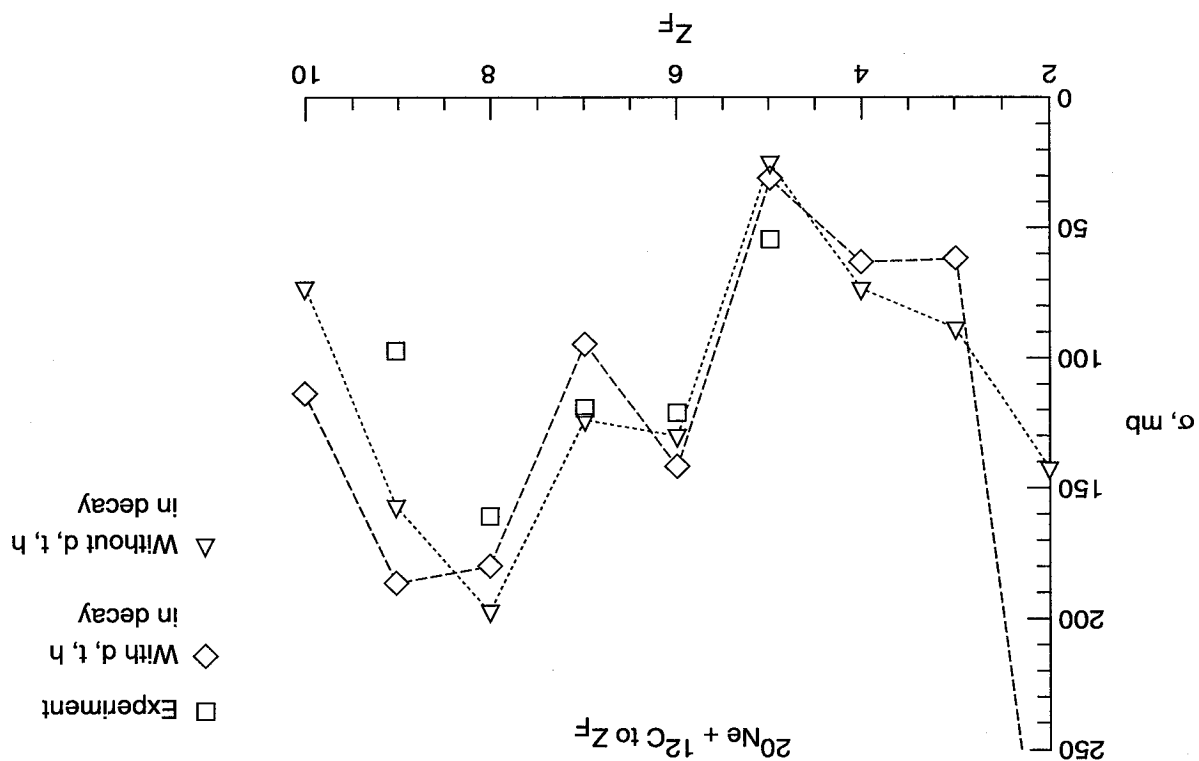
(a) Elemental production.

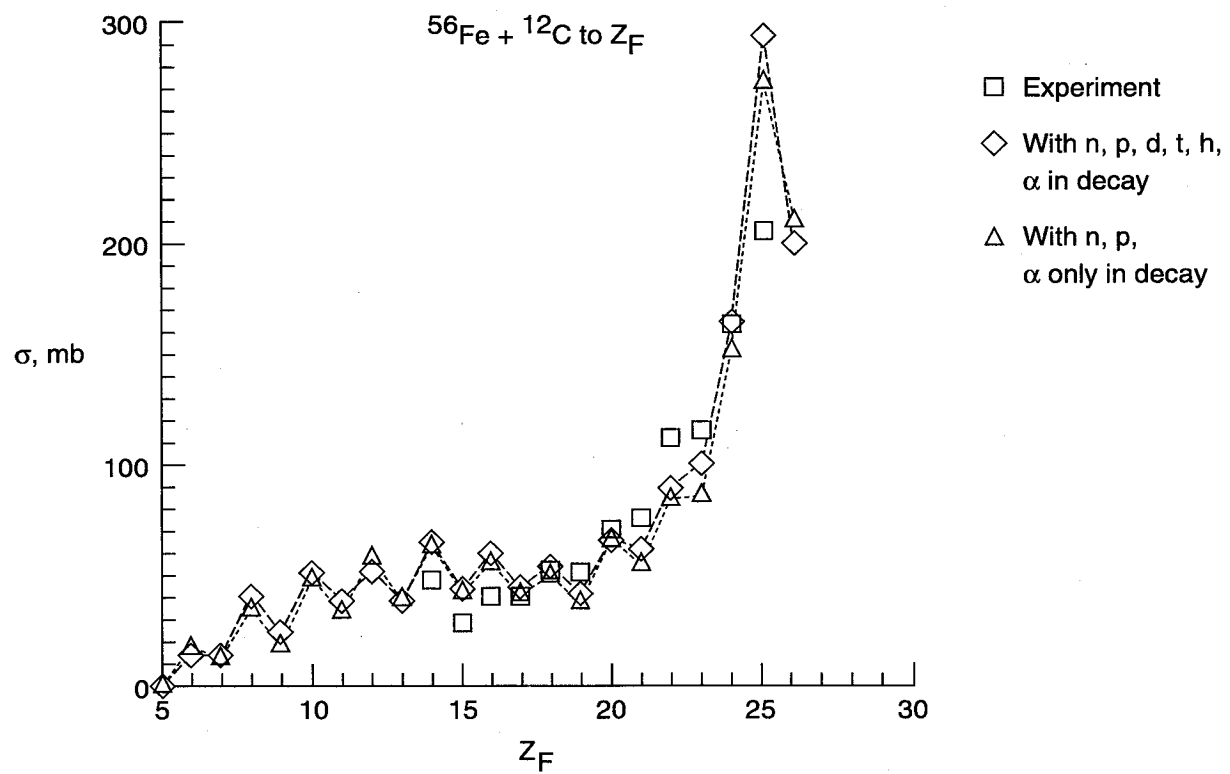


(b) Mass production.

Figure 9. Excitation energy cross section profiles for $^{32}\text{S} + ^{12}\text{C}$ at 3.65 GeV/amu.

Figure 10. Calculations of elemental production for three or six decay particles considered in evapora-

(b) Cross sections for $^{49}\text{Ar} + ^{12}\text{C}$ at 1.65 GeV/amu.(a) Cross sections for $^{20}\text{Ne} + ^{12}\text{C}$ at 0.6 GeV/amu.



(c) Cross sections for $^{56}\text{Fe} + ^{12}\text{C}$ at 0.52 GeV/amu.

Figure 10. Concluded.

REPORT DOCUMENTATION PAGE			Form Approved OMB No. 0704-0188	
Public reporting burden for this collection of information is estimated to average 1 hour per response, including the time for reviewing instructions, searching existing data sources, gathering and maintaining the data needed, and completing and reviewing the collection of information. Send comments regarding this burden estimate or any other aspect of this collection of information, including suggestions for reducing this burden, to Washington Headquarters Services, Directorate for Information Operations and Reports, 1215 Jefferson Davis Highway, Suite 1204, Arlington, VA 22202-4302, and to the Office of Management and Budget, Paperwork Reduction Project (0704-0188), Washington, DC 20503.				
1. AGENCY USE ONLY (Leave blank)	2. REPORT DATE October 1996	3. REPORT TYPE AND DATES COVERED Technical Paper		
4. TITLE AND SUBTITLE Study of Analytic Statistical Model for Decay of Light and Medium Mass Nuclei in Nuclear Fragmentation		5. FUNDING NUMBERS WU 199-45-16-11		
6. AUTHOR(S) Francis A. Cucinotta and John W. Wilson				
7. PERFORMING ORGANIZATION NAME(S) AND ADDRESS(ES) NASA Langley Research Center Hampton, VA 23681-0001		8. PERFORMING ORGANIZATION REPORT NUMBER L-17542		
9. SPONSORING/MONITORING AGENCY NAME(S) AND ADDRESS(ES) National Aeronautics and Space Administration Washington, DC 20546-0001		10. SPONSORING/MONITORING AGENCY REPORT NUMBER NASA TP-3594		
11. SUPPLEMENTARY NOTES				
12a. DISTRIBUTION/AVAILABILITY STATEMENT Unclassified-Unlimited Subject Category 73 Availability: NASA CASI (301) 621-0390		12b. DISTRIBUTION CODE		
13. ABSTRACT (Maximum 200 words) The angular momentum independent statistical decay model is often applied using a Monte-Carlo simulation to describe the decay of prefragment nuclei in heavy ion reactions. This paper presents an analytical approach to the decay problem of nuclei with mass number less than 60, which is important for galactic cosmic ray (GCR) studies. This decay problem of nuclei with mass number less than 60 incorporates well-known levels of the lightest nuclei ($A < 11$) to improve convergence and accuracy. A sensitivity study of the model level density function is used to determine the impact on mass and charge distributions in nuclear fragmentation. This angular momentum independent statistical decay model also describes the momentum and energy distribution of emitted particles (n, p, d, t, h , and α) from a prefragment nucleus.				
14. SUBJECT TERMS Heavy ions; Nuclear fragmentation; Galactic cosmic rays		15. NUMBER OF PAGES 26		
		16. PRICE CODE A03		
17. SECURITY CLASSIFICATION OF REPORT Unclassified	18. SECURITY CLASSIFICATION OF THIS PAGE Unclassified	19. SECURITY CLASSIFICATION OF ABSTRACT Unclassified	20. LIMITATION OF ABSTRACT	